Bond Response in Structural Concrete with Corroded Steel Bars. Experimental Results

M. Prieto, P. Tanner and C. Andrade

Instituto Eduardo Torroja de Ciencias de la Construcción (IETcc-CSIC),
Serrano Galvache, 4, 28033 Madrid, Spain.

Abstract The growing interest in upgrading existing reinforced concrete structures or extending their service life, and in ensuring greater durability in new designs, has led to a need for resistance models that take deterioration processes into account to verify structural safety. Bond activation between reinforcing steel and concrete is of cardinal importance in this context. A number of experimental studies have been conducted in recent years on bond failure, which normally leads to brittle behaviour. The findings have diverged rather widely, however, due primarily to differing test conditions. The present paper presents an experimental programme for eccentric pull-out tests in which specimens were subjected to both accelerated and natural corrosion in an attempt to surmount these inconsistencies. It also introduces an embedded fibre-optic sensing system with corrosion-resistant fibre Bragg grating sensors and discusses some of the findings.

Introduction

Resistance

Strength models that take deterioration processes into consideration must be developed to verify the structural safety of new and existing construction. The strength of corroded reinforced concrete structures depends on the cross-section of the corroded steel, its stress-strain diagram, the bond between it and the concrete and corrosion-induced concrete cracking. Since the failure of force transfer between the reinforcement and the surrounding concrete normally leads to brittle behaviour, bond is one of the most important aspects to consider and it is the basis of the structural performance of reinforced concrete. A number of experimental and numerical studies on corroded steel bar bonding have been conducted in recent

years (e.g., [1, 2, 3, 4, 11, 12]), although the differences in test conditions have led to widely dispersed results. In an attempt to overcome these inconsistencies, in the present study eccentric pull-out tests were conducted in which specimens were subjected to accelerated and natural corrosion, to study bonding in structural concrete with corroded steel bars. The experimental procedure is described, including the data acquisition by means of an embedded fibre-optic sensing system with corrosion-resistant fibre Bragg grating sensor. Some of the results forthcoming to date are also discussed.

Force Transfer between Corrosion-Free Reinforcement and Concrete

Interface properties

Bonding materializes in structural concrete due to the contact between the steel reinforcement and the concrete. Therefore, bond response may vary with the properties of this interface. Depending on these properties, three different mechanisms may be come into play: adhesion (where slipping is relatively minor), friction (prevalent when confinement pressure is present or in the unloading phase) and rib action (present only where ribbed bars are used). The former two influence bond strength in plain bars, while the third determines the maximum bond strength that can be attained for ribbed bars. Depending on rib geometry, moreover, different failure modes can be found [6]: pull-out, splitting-induced pull-out accompanied by crushing and/or shearing-off and splitting accompanied by slip on the rib faces.

Anchorage of reinforcing bars

Where ribbed bars are used, once the stress exceeds the bond strength afforded by adhesion and friction, force is transferred across the ribs. For a simplified description of the internal forces at failure, the actual stress field can be regarded to be an axisymmetric stress field [7] in which the diagonal deviation of the compression field is absorbed by a concrete tension ring (Figure 1a) or stirrups (Figure 1b). Anchorage fails either because the concrete tension ring fails or the stirrups yield.

Bond strength

In the absence of stirrups, for ribbed bars the maximum bond strength is achieved due to the ribs and depends on anchorage length, concrete tensile strength and the thickness of the tension ring. A theoretical assessment of the stress field in Figure 1a [7] found a linear relationship between bond strength and ring thickness.

The present study attempts to verify whether this relationship is suitable for the test set-up used in this work and to determine bonding of corroded steel bars in the absence of stirrup for different degrees of corrosion.
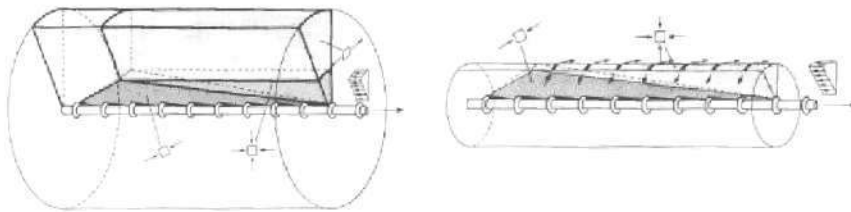

Figure 1. Stress field describing the stress state in the anchorage zone: a) diagonal deviation absorbed by concrete tension ring and b) diagonal deviation absorbed by confining reinforcement [7].

Previous Studies on Bond with Corroded Steel Bars

Overview

Corrosion can affect bond development and with it the transfer of longitudinal stresses. Factors that affect bond strength include the weakening of the steel bar confinement due to cracking on the concrete cover and/or stirrup corrosion, development of corrosion products at the interface, and, in the case of ribbed bars, reduction of the relative rib area due to cross-section loss in the steel. The effect of corrosion on the steel-to-concrete bond has been studied both experimentally and numerically. Numerical studies are beyond the scope of this paper at this time. A number of experimental studies involving tests on ribbed bars without stirrups are briefly reviewed below.

Experimental studies

A wide variety of test specimens with intact and corroded steel have been used to study bond behaviour. While the number is far too large to be analyzed here, the importance of choosing the right size and shape of specimen and suitable corrosion acceleration techniques in bond testing cannot be overstated.

Due to the fact that natural corrosion needs a long time to develop, current is usually applied to accelerate the process. In a previous study [10] was suggested to use a maximum current density of 100-200 $\mu A/cm^2$. Furthermore, a comparison of findings using current densities ranging from 3 to 100 $\mu A/cm^2$ [10] showed that the

higher the current density, the higher was the penetration rate needed to achieve a given crack width.

The use by some authors [2, 4, 12, 13, 14] of current densities higher than the maxima found under real conditions may have yielded bond behaviour values that may not be representative of field conditions.

Specifically, some of these studies [4, 12, 14] used short specimens with a length-to-bar diameter ratio of $L/\phi \leq 5$ for the bond strength trials. These specimens are useful for studying local bond-slip behaviour, and slip and bond stresses can be regarded to be constant along the length of the bar. Long specimens ($L/\phi > 5$) have also been used [1, 2, 3, 13] for bond tests. These specimens provide helpful information on anchorage behaviour and bond stress distribution along the embedded length of the bar, while serving as a reference for FE modelling. The main focus of the present study is bond stress behaviour along this embedded length, using long specimens.

Test Planning

Pull-out tests

Traditional bond tests measure bond strength at pull-out-induced failure. In pull-out tests, the bar is centrally embedded, and the c/ϕ ratios are so high that failure normally takes place because of pull-out. In beam tests, pull-out failure is usually the result of high amount of transverse reinforcement.

A bond test has been developed [15] and used [1, 3] that reproduces the situation of a reinforcing bar in a beam with a variable bending moment and a constant shear force. The advantages of this test are that, in addition to simulating the actual condition of the bars, it can be used to reproduce splitting failures, and it accommodates testing of four bars in each specimen and comparison of the results by bar location (top and bottom casting position). For all these reasons, this was the test set-up chosen for the present research. Compared to previous studies, in this case, an additional PVC pipe was placed on the load side of the specimen to prevent undesired boundary effects. The bond test set-up is shown in the figure below.
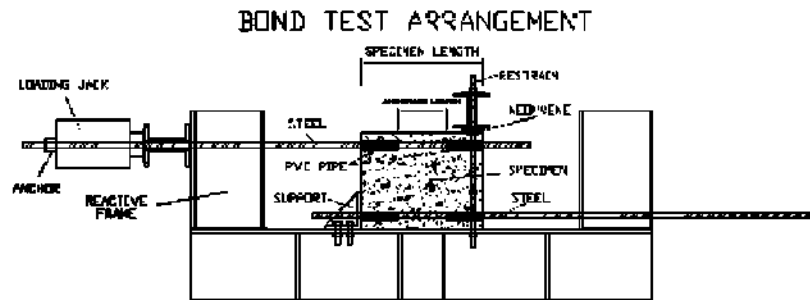
BOND TEST ARRANGEMENT

Figure 2. Test set-up

Specimens

Specimens with a 400x400-mm cross-section and 500 or 600 mm long, depending on bar diameter, were used (Figure 3). Long specimens were used and the same length-to-diameter ratio was maintained throughout, namely, anchorage length was 11ϕ in all specimens thus preventing the steel from yielding. To prevent pressure induced by the test set-up and load-side boundary effects, the bars were protected with an embedded PVC pipe on both sides of the specimen. The ratios used for the concrete tension ring ranged from 2.1 to 4. The concrete specimens were reinforced at the corners with four bars measuring 10, 12 or 25 mm in diameter. Two bars were placed at the top and two at the bottom (casting position). The following figures show the test specimens with and without stirrups.
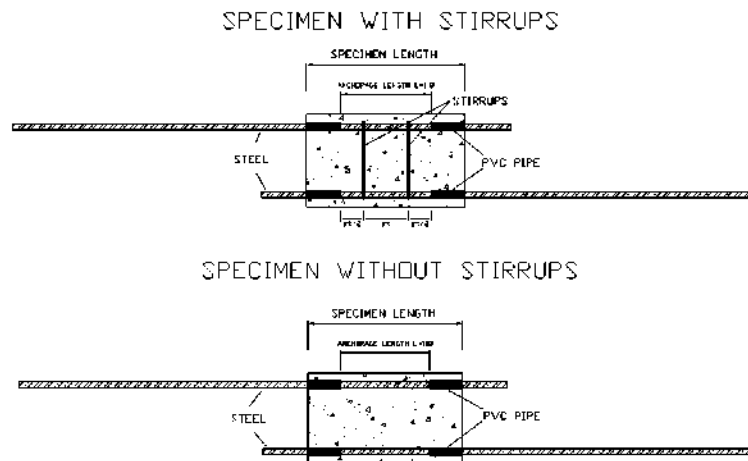
SPECIMEN WITH STIRRUPS

SPECIMEN WITHOUT STIRRUPS

Figure 3. Set-up for specimens with and without stirrups

Data acquisition

The mechanical properties of the materials, i.e., concrete splitting and compressive strength and steel yield and ultimate strength, were found at the same age as when the eccentric pull-out tests were conducted. The following data were acquired during these tests:

− Relative bar slip measurement. Three linear variable displacement transducers (LVDT) with a maximum range of 6 mm. were placed on each side of the specimen.
− Steel strain measurement along the anchorage length. With the fibre optic system used, three Fibre Bragg grating (FBG) strain gauges were positioned along the anchorage length. A Micron Optics sm130 optical sensing interrogator with a wavelength range of 1 510 to 1 590 nm was used for measurements.
− Crack width measurement. Three omega-shaped displacement transducers with a range of ±2 mm were placed on the concrete surface in the same position as the FBG to monitor crack width.
− Load measurement. A 310-kN loading jack was used. The load was applied at a constant 3 kN/min in several steps.

In this investigation, an embedded fibre-optic sensing system with fibre Bragg grating sensors (FBGs) was used to measure strain along the length of the embedded bar, in order to monitor the load transfer from the bar to the concrete. This type of sensor was chosen over electrical sensors because its small dimensions allow fibre embedment without affecting the mechanical behaviour to be measured. Moreover, FBGs have excellent resolution and range and can be multiplexed, i.e., several sensors can be used in the same fibre. The fibres themselves also act as both sensing elements and a signal propagation conduit. Finally, one of the most important reasons for using FBGs is that they are water- and corrosion-resistant and impervious to harsh weather conditions, electromagnetic interference and ground loops.
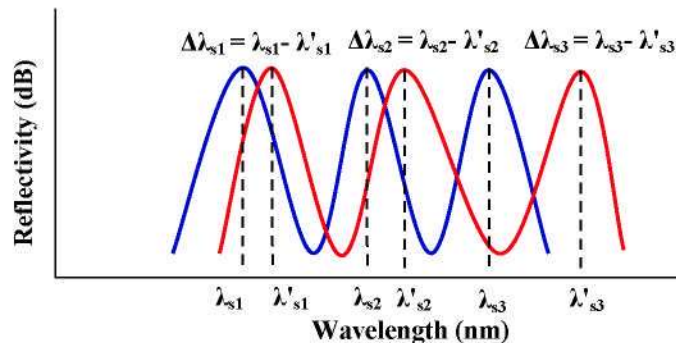

Figure 4. Variation in peak reflectivity with applied strain according to multiplexed FBG system used in this study

When strain is induced in an FBG sensor, either due to mechanical stress, thermal expansion or a combination of the two, its grating pitch changes in such a way that its reflected wavelength varies in proportion to the strain. Strain can therefore be found by measuring the variation in the reflected wavelength.
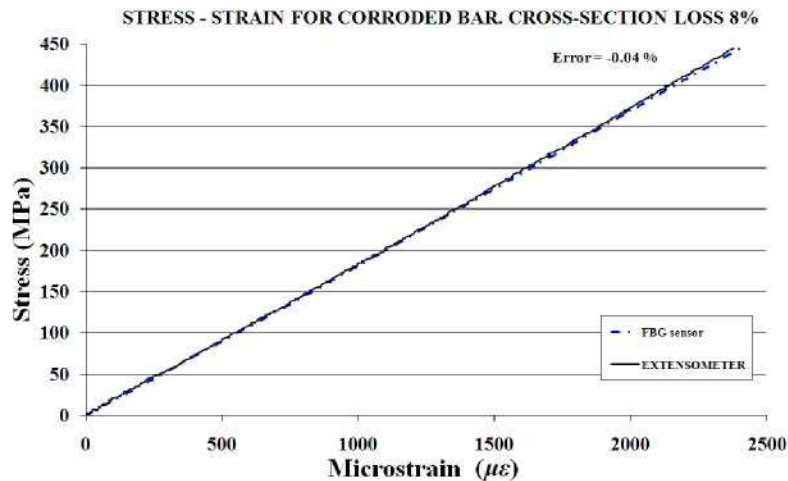

Figure 5. FBG sensor versus conventional strain gauge measurements during a tensile test on a corroded bar

In this investigation, preliminary tensile tests were conducted on non-corroded and corroded bars to perfect a fibre optic system for measuring steel strain in corroded bars during the eccentric pull-out test. The optical fibre was secured with epoxy resin in a 1x2-mm slot in the longitudinal rib of the bar along the anchorage length. The measurements taken with the fibre are compared to the results found with an ordinary strain gauge in the following figure.

Test programme

Eight specimens were prepared for this study, three measuring 400x400x500 and five 400x400x600. Two of these were control specimens, not exposed to corrosion; five were prepared with corrosion levels ranging from 2 to 12%, and one was exposed to natural corrosion, likewise as a control. The characteristics of the experimental programme are shown in the following table:

Parameter	Value
Type of test	Eccentric pull-out
Type of bars	Ribbed bars
Nominal steel yield strength	500 MPa
Concrete compressive strength	25 to 40 MPa

Type of splicing	No splicing
Bar position	Top and bottom
Anchorage length	11ϕ Straight
Thickness of concrete tension ring (a/ϕ)	2,1, 3 and 4
Longitudinal bar diameter	10, 12 and 25 mm
Stirrup diameter	10 mm
Confinement	None, stirrups and external pressure
Type of corrosion	Accelerated and natural
Corrosion-induced cross-section loss	0%, 2%, 8%, 12%

Testing

Three concrete mix compositions were used to obtain compressive strengths ranging from 25 to 40 MPa. To induce corrosion, 3% NaCl by weight of cement was added to the concrete mix for the specimens used for natural and accelerated corrosion. After curing in damp burlap for seven days, the specimens were stored under no special temperature or humidity conditions to an age of 28 days to ensure that the material had reached a reasonable compressive and splitting strength before proceeding to accelerated corrosion. The control specimens not exposed to corrosion were stored under the same conditions until they were tested. For eighteen months, while this study is ongoing, the natural corrosion specimen will be subjected to wet-dry cycles for comparison to the accelerated corrosion procedure. In this specimen, corrosion rate is periodically measured by means of a corrosion rate meter, Gecor 8, to monitor the steel cross section loss along time.

Further to a procedure described elsewhere [1, 3, 9], corrosion was accelerated in the other five specimens by applying a constant current density with a galvanostat through counter-electrodes placed on the concrete surface of the specimen. A wet sponge was used to produce electrical contact between the counter-electrodes and the specimen. A current density of 100 μA/cm^2 was used in two of the specimens, and of 200 μA/cm^2 in the other three. Two current densities were used to compare the findings to the results for the control specimen exposed to natural corrosion. With only two exceptions [1, 3] that used the same value, the current densities applied in this study were much lower than cited for bond tests in the literature.

Results and Discusion

Only the maximum bond strength values found to date are shown in this paper. A linear regression analysis was performed to confirm, for the test set up used in this work, the relationship between normalized bond strength (maximum bond strength divided by concrete tensile strength) and the ratio between the radius of the

concrete tension ring, a, and the bar diameter, ϕ, as shown in the graph below. The data used to plot this graph were taken from the literature (beam tests [7], compiled test findings [8], pull-out tests on non-corroded specimens [1, 2, 3, 4]) and the results of the pull-out tests on non-corroded specimens conducted for the present study.
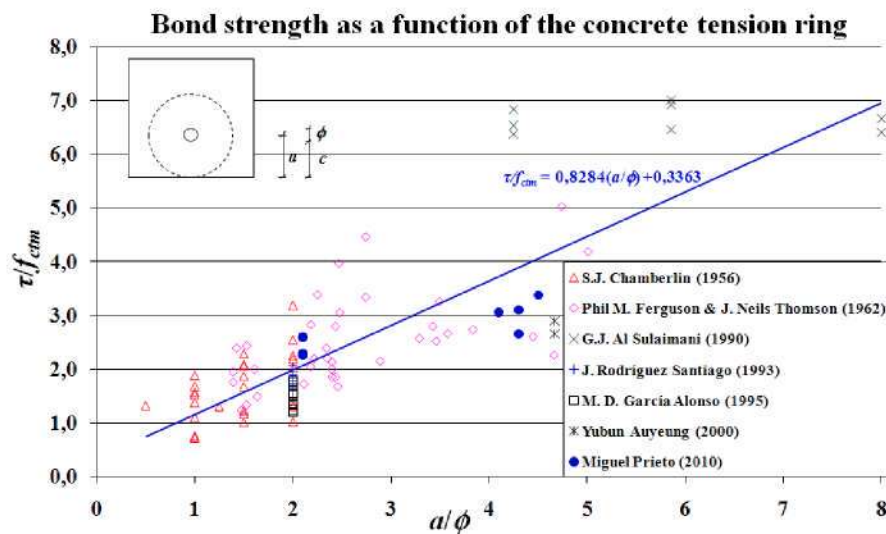

Figure 6. Normalized bond strength versus concrete tension ring thickness

The corroded steel bar bond test results (without stirrups) reported in the literature [1, 2, 3, 4, 12] and the values observed in the present study to date were evaluated also to determine the existence or otherwise of a relationship such as shown in Figure 6.

Normalized bond strength for non corroded bars, for corroded bars with cross section loss up to 5% and cross section loss between 5 and 10%, is plotted against tension ring thickness in Figure 7. Linear regression analysis was performed for the results available from literature for each of these categories. Furthermore, distribution fitting taking into account the number of test results was performed, showing the log-normal distribution the best fit. The results of the present investigation to date are within the scatter observed for each category of results wich, on the other hand, is rather wide with coefficients of variation (CoV) of 0.23 for non corroded bars, 0.78 for corroded bars with cross section loss up to 5% and 0.82 for corroded bars with cross section loss between 5 and 10%. This dispersion is typical of bond tests due to the large number of influencing variables.
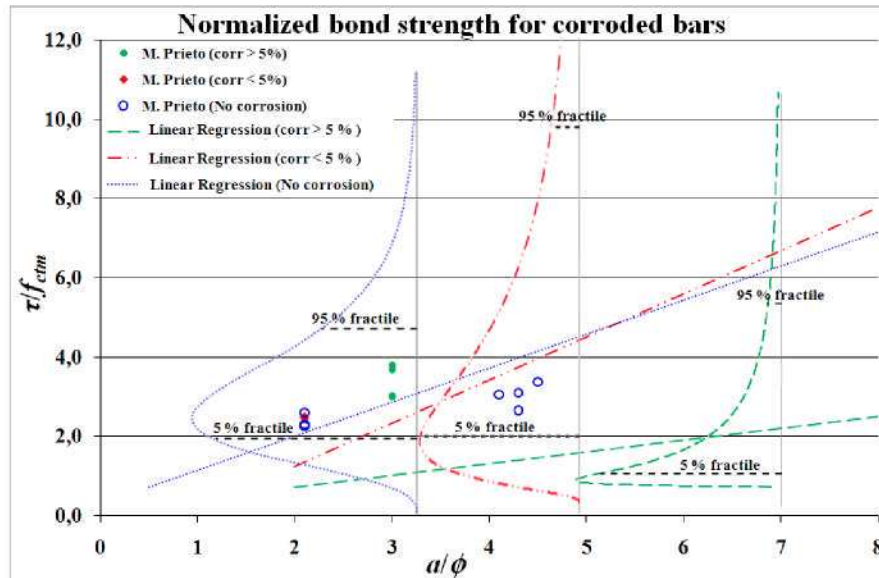
Figure 7. Normalized bond strength for corroded bars versus concrete tension ring thickness and degree of corrosion

The comparison of the results from the present study to the findings reported by other authors [1, 2], in which the same accelerated corrosion procedure, long specimens and nearly the same test set-up were used, show for nearly the same concrete tension ring ratio a clearly higher normalized bond strength than the results reported in the two papers cited. These differences may be due to the variations in the test set-up: in the present study, an additional PVC pipe was used to prevent undesired boundary effects on the load side.

Final Remarks

This paper discusses an experimental programme of eccentric pull-out tests with specimens exposed to accelerated and natural corrosion. An embedded fibre-optic sensing system with corrosion-resistant fibre Bragg grating sensors, developed to measure strain along the anchorage length of corroded bars, is also introduced. Some of the experimental results found to date are given and compared to the findings reported by other authors in terms of normalized bond strength plotted against concrete tension ring thickness and degree of corrosion. Although the results are widely scattered, typical of bond tests due to the large number of influencing variables, a relationship between normalized bond strength for corroded bars without stirrups and concrete tension ring thickness for each category of corrosion has emerged. The detailed analysis of the fibre optic measurements of load transfer should contribute to a better understanding of bond

mechanics in case of corrosion. Furthermore, the results for the specimens not yet tested (three exposed to accelerated and one to natural corrosion), together with the findings presently available and a broader parametric study with a numerical model based on these tests, is expected to lead to a fuller explanation of bond behaviour.

Acknowledgment

References

[1] Garcia Alonso, M.D. (1995). *Aportaciones al comportamiento resistente de estructuras de hormigón armado afectadas por la corrosión de sus armaduras*, Thesis of Polytechnical University of Madrid (UPM), E.T.S.A., Madrid.

[2] Auyeung, Y. and Balaguru, P. and Chung, L. (2000), *ACI Structural Journal*, vol. 97, n. 2, p. 214.

[3] Rodriguez, J. et al. (1995). *The residual service life of reinforced concrete structures. Task 3.2. Relation between corrosion and bond deterioration.* Brite Euram Project BREU-CT-0591.

[4] Al-Sulaimani, G.J. and Kaleemullah, M. and Basunbul, I.A. and Rasheeduzzafar (1990), *ACI Structural Journal*, vol. 87, n. 2, p 220.

[5] Fernandez, M. and Hars, E. and Muttoni, A. (2005). *Bond mechanics in structural concrete. Theoretical model and experimental results*, Draft, IS-BETON, Ecole Polytechnique Fédérale de Lausanne.

[6] FIB (2000). *Fib bulletin 10: Bond of reinforcement in concrete*, Lausanne.

[7] Muttoni, A. and Schwartz, J. and Thürlimann, B. (1997). *Design of Concrete Structures with Stress Fields*, Birkhäuser Verlag, Berlin.

[8] Chamberlin, S. J. (1956). *Proceedings of Journal of the American Concrete Institute*, vol. 53, n. 6, p. 113.

[9] Andrade, C. and Alonso, C. and Molina F. J. (1993). *Materials and Structures*, vol. 26, p. 453.

[10] Andrade, C. and Alonso, C. (1996). *Construction and Building Materials*, vol. 10, n. 5, p. 315.

[11] Alonso, C. and Andrade, C. and Rodriguez, J. and Diez, M.J. (1998). *Materials and Structures*, vol. 31, n. 7, p. 435.

[12] Fang, C. and Lundgren, K. and Chen, L. and Zhu, C. (2004). *Cement and Concrete Research*, vol. 34, n. 11, p. 2159.

[13] Almusallam, A.A. and Al-Ghatani, A.S. and Aziz, A.R. and Rasheeduzzafar (1996), *Construction and Building Materials*, vol. 10, n. 2, p. 123.

[14] Cabrera, J.G. (1996), *Cement and Concrete Composites*, vol. 18, n. 1, p. 47.

[15] Chana, P.S. (1990), *Magazine of Concrete Research*, vol. 42, n. 151, p. 83.